Plant Physiology and Biochemistry 142 (2019) 94–105

Contents lists available at ScienceDirect

Plant Physiology and Biochemistry

journal homepage: www.elsevier.com/locate/plaphy

Research article

Evaluation, characterization, expression profiling, and functional analysis of *DXS* and *DXR* genes of *Populus trichocarpa*

Chen Xu[a,b,1], Hui Wei[a,1], Ali Movahedi[a,1], Weibo Sun[a,1], Xiaoxing Ma[a], Dawei Li[a], Tongming Yin[a], Qiang Zhuge[a,*]

[a] Co-Innovation Center for Sustainable Forestry in Southern China, Key Laboratory of Forest Genetics & Biotechnology, Ministry of Education, Nanjing Forestry University. Nanjing, 210037, China
[b] Nanjing Key Laboratory of Quality and Safety of Agricultural Products, Nanjing Xiaozhuang University, Nanjing, 211171, China

ARTICLE INFO

Keywords:
Populus trichocarpa
DXS
DXR
HPLC–MS/MS
Expression

ABSTRACT

1-Deoxy-D-xylulose-5-phosphate synthasse (DXS) and 1-deoxy-D-xylulose-5-phosphate reductoisomerase (DXR) are key enzymes in terpenoid biosynthesis. DXS catalyzes the formation of 1-deoxy-D-xylulose 5-phosphate (DXP) from pyruvate and D-glyceraldehyde-3-phosphate. DXR catalyzes the formation of 2-C-methyl-D-erythritol 4-phosphate (MEP) from DXP. Previous studies of the *DXS* and *DXR* genes have focused on herbs, such as *Arabidopsis thaliana*, *Salvia miltiorrhiza*, and *Amomum villosum*, but few studies have been conducted on woody plants. For that reason, we chose *Populus trichocarpa* as a model woody plant for investigating the *DXS* and *DXR* genes. *PtDXS* exhibited the highest expression level in leaves and the lowest expression in roots. *PtDXR* showed maximum expression in young leaves, and the lowest expression in mature leaves. The expression profiles revealed by RT-PCR following different elicitor treatments such as abscisic acid, NaCl, PEG_{6000}, H_2O_2, and cold stress showed that *PtDXS* and *PtDXR* were elicitor-responsive genes. Our results showed that the *PtDXS* gene exhibited diurnal changes, but *PtDXR* did not. Moreover, overexpression of *PtDXR* in transgenic poplars improved tolerance to abiotic and biotic stresses. Those results showed that the *PtDXR* encoded a functional protein, and widely participates in plant growth and development, stress physiological process.

1. Introduction

The biosynthesis of terpenoids requires common precursor substances, including isopentenyl diphosphate (IPP) and its isomer dimethylallyl diphosphate (DMAPP). In plants, there are two distinct pathways for isoprenoid biosynthesis (Lange et al., 2001). One is the plastid-located 2-C-methyl-D-erythritol-4-phosphate (MEP) pathway and the other is the cytoplast-located mevalonic acid (MVA) pathway (Eisenreich et al., 1998; Lichtenthaler, 1999; Rohmer, 1999; Shen et al., 2006). The first two rate-limiting enzymes in the MEP pathway are 1-deoxy-D-xylulose-5-phosphate synthase (DXS) and 1-deoxy-D-xylulose-5-phosphate reductoisomerase (DXR). The first major step involves DXS-dependent catalysis of pyruvate and D-glyceraldehyde-3-phosphate to form 1-deoxy-D-xylulose-5-phosphate (DXP) (Lois et al., 2000). The second step is catalyzed by DXR and generates MEP, followed by several enzymatic reactions to produce precursors of IPP and DMAPP (Lange et al., 1999; Eisenreich et al., 2004). The genes encoding DXS have also been isolated from several plants, such as *Arabidopsis thaliana* (Estevez et al., 2001) *Croton stellatopilosus* Wungsintaweekul et al. (2008); *Zea mays* (Hans et al., 2004), *Ginkgo biloba* (Gong et al., 2005), *Salvia miltiorrhiza* (Wu et al., 2009), and *Camptotheca acuminata* (Yao et al., 2008). A large number of studies have suggested that both the *DXS* and *DXR* genes can regulate flux through the MEP pathway and influence accumulation of downstream products. Studies on the overexpression of *DXS* and *DXR* in *A. thaliana* and tomato (Estevez et al., 2001; Enfissi et al., 2005; Yang et al., 2012) have been performed to determine whether the step catalyzed by DXS or DXR is the limiting step for the biosynthesis of plastidial isoprenoids in plant cells. Furthermore, overexpression of *DXS* and *DXR* in prokaryotes has been shown to result in a drastic increase in diterpene yield in transgenic bacteria (Morrone et al., 2010). DXS and *DXR* genes from *Catharanthus roseus* are overexpressed in hairy roots, indicating that DXS and DXR can increase accumulation of terpenoid indole alkaloids (Peebles et al., 2011). Furthermore, the first report of MEP pathway regulation in the

* Corresponding author. Co-Innovation Center for Sustainable Forestry in Southern China, Key Laboratory of Forest Genetics and Biotechnology, Ministry of Education, Nanjing Forestry University, Nanjing, 210037, China.
E-mail address: qzhuge@njfu.edu.cn (Q. Zhuge).
[1] These authors are contributed equally as the first author.

https://doi.org/10.1016/j.plaphy.2019.05.034
Received 14 February 2019; Received in revised form 31 May 2019; Accepted 31 May 2019
Available online 10 June 2019

colonization of wheat, maize, rice and barley by mycorrhizal fungi involved activation of DXS and DXR. The plant–pathogen interaction was reported to involve developmental or environmental regulation. The result demonstrated that the *DXS* expression level changes after root infection by mycorrhizal fungi (Walter et al., 2010). *MtDXS2* was highly expressed in the roots of *Medicago truncatula* infected by arbuscular mycorrhizal fungi (Zhang et al., 2009; Floss et al., 2010). The occurrence of late blight in potato is accompanied by decreased *DXS* expression, which leads to reduced levels of disease-resistant isoprenes (Henriquez et al., 2016). In this experiment, we used the pathogen *Septotis populiperda* to infect poplar leaves over-expressing the *DXR* gene. Taken together, these studies suggest that both DXS and DXR are rate-limiting enzymes involved in a variety of biological reactions. In addition, DXS and DXR are also potential regulatory enzymes for manipulating biosynthetic pathways to produce isoprenoids of commercial significance.

Although there have been numerous studies on the *DXS* and *DXR* genes, there has been little molecular research on these genes in *Populus trichocarpa*. In this study, we performed molecular cloning, characterization, and functional analysis of the *DXS* and *DXR* genes of *P. trichocarpa*. We investigated the functions of these enzymes and their expression patterns in different tissues and under abiotic stresses and discovered diurnal variations in the expression of the *DXS* and *DXR* genes. Furthermore, we found that overexpression of *PtDXR* enhances tolerance to salt and drought as well as *Septotis populiperda* in transgenic poplars.

2. Materials and methods

2.1. Materials

We choose 3-month-old seedlings of *P. trichocarpa*, which were grown on sterile half-strength Murashige and Skoog (1962) medium (pH 5.8). Total RNA was extracted from *P. trichocarpa* plants. *Escherichia coli* Top 10 cells (maintained in our laboratory) were used for cloning and propagation, while *E. coli* BL21 (DE3) cells (Novagen, USA) were used for prokaryotic expression. Polymerase chain reaction (PCR) cleanup kits were purchased from Takara Biotechnology Co., Ltd. (Japan). Primer synthesis and DNA sequencing were performed by Invitrogen Biotechnological Company (Shanghai, China).

2.2. RNA isolation and cDNA synthesis

The Biomiga Miniprep kit was used to extract total RNA. In addition, cDNA was synthesized using MMLV reverse transcriptase (Takara Biotechnology Co., Ltd.) (Movahedi et al., 2015). This reverse transcription reaction system contained the following reagents: 1 μg cDNA template, 1 μl oligo (dT), 1 μl 10 mM dNTPs, 0.5 μl RNase inhibitor, 1 μl MMLV reverse transcriptase, 4 μl MMLV reverse transcriptase buffer, and ddH_2O to a final volume of 20 μl. The reaction was performed as follows: 65 °C for 10 min, on ice for 3 min, 42 °C for 1 h, 70 °C for 15 min, and a final incubation on ice for 3 min.

2.3. Cloning of the open PtDXS and PtDXR genes

To identify the *DXS* and *DXR* genes, the National Center for Biotechnology Information (NCBI) was used to find the sequences of *DXS* and *DXR* genes of *Populus trichocarpa*. The PCR reaction was performed in tubes containing 2.0 μl template cDNA, 1.5 μl each of forward and reverse primers, 5.0 μl 10 × PCR buffer (Mg^{2+} plus), 4 μl dNTPs, and 0.5 μl rTaq DNA polymerase (Takara Biotechnology Co., Ltd.). The reaction was performed as follows: 95 °C for 7 min, 35 cycles of 95 °C for 30 s, 56 °C for 30 s, and 72 °C for 2 min (DXS) or 1.5 min (DXR), and finally, 72 °C for 10 min. Next, the target bands were excised, gel extraction reagent was added, and the bands were purified. The purified products were cloned into the PEASY-T3 vector, and transformed into *E. coli* TransTI. Based on the color reaction system using X-Gal and isopropyl β-D-1-thiogalactopyranoside (IPTG) as well as PCR analysis, the positive clones were isolated and sequenced (Invitrogen).

2.4. Construction of the PET-28a fused expression vector

According to the sequences of *PtDXS* and *PtDXR* genes and the vector restriction sites, we designed the primers fused restriction sites. The PCR reaction mixture as follow: 5.0 μl 10 × PCR buffer (Mg^{2+} plus), 4.0 μl 2.5 mmol dNTPs, 1.5 μl primers for the ligase restriction site, 2.0 ml PEASY-T3 vector including PtDXS and PtDXR as template, 0.5 μl 5 U Pfu enzyme, and 35.5 μl ddH_2O. The *PtDXS* gene was cloned into the expression vector pET-28a between the *Bam*HI and NotI sites.

2.5. Fesed protein expression and purification

After sequencing, the recombinant plasmids pET-28a-PtDXS and pET-28a-PtDXR were transformed into *E. coli* BL21 (DE3). Positive recombinant clones cultured in 1 L of LB to achieve an optical density (OD) of 0.6–0.8 at 600 nm. Also, 1 mM IPTG was added to the cultured solutions and *E. coli* BL21 (DE3) containing plasmids pET-28a-PtDXS and pET-28a-PtDXR were maintained at 220 rpm for 4 h at 37 °C. In addition, we use 12% sodium dodecyl sulfate polyacrylamide gel electrophoresis (SDS-PAGE) to analyze the un-induced and induced solutions.

According to the analysis of 12% SDS-PAGE, we found that the target proteins were expressed in precipitation. Therefore, we next performed the operations of denaturation and renaturation. The collected precipitate was first washed three times with inclusion body washing solution 1 (20 mM Tris, 1 mM EDTA, 2 M urea, 1 M NaCl, and 1% Triton X-100, pH 8.1), followed by two washes with inclusion body washing solution 2 (20 mM Tris, 1 mM EDTA, 4 M urea, 1 M NaCl, and 1% Triton X-100, pH 8.1). The precipitate was then washed once with inclusion body washing solution 3 (20 mM Tris, 1 mM EDTA, 6 M urea, 1 M NaCl, and 1% Triton X-100, pH 8.1). Finally, the precipitate was collected and dissolved in inclusion body dissolving solution (20 mM Tris, 1 mM EDTA, 8 M urea, 1 M NaCl, and 1% Triton X-100, pH 8.1). The collected degeneration solution was stored for 48 h at 4 °C and centrifuged at 13,000 × *g* for 20 min at 4 °C. The inclusion bodies dissolved in solution were added dropwise to 20 mM Tris (pH 8.1). Renaturation buffer (4–0.5 M urea, 0.5 M NaCl, 10 mM Tris, 0.5 mM EDTA, 1 mM L-arginine, 1 mM reduced L-glutathione, 0.2 mM oxidized L-glutathione, and 5 mM DTT, pH 8.1) was gradually added in a series of four dilutions. The target protein solutions were transferred to a dialysis bag and incubated overnight at 4 °C in dialysis buffer. During dialysis, the concentration was reduced and bacterial lysis buffer (2 mM KH_2PO_4, 4 mM Na_2HPO_4, 3 mM KCl, and 150 mM NaCl) was used as the final dialysis buffer. The target protein was analyzed using 12% SDS-PAGE. Mixed protein was applied to a Ni + -NTA-chelating column equilibrated with Ni + -NTA binding buffer (20 mM Tris-base, 500 mM NaCl, and 20 mM imidazole). After washing with Ni + -NTA wash buffer until the baseline absorbance was reached, the column was washed with 250 mM imidazole in buffer (20 mM Tris-HCl and 500 mM NaCl, pH 8.1) at a flow rate of 1 ml/min. The fractions were collected and analyzed with 12% SDS-PAGE. Following overnight dialysis at 4 °C with phosphate-buffered saline (PBS), the protein was lyophilized.

2.6. Western blotting

Western blotting was performed as described by Sambrook et al. (1989) with rabbit anti-His polyclonal antibody made in our laboratory as the primary antibody and peroxidase-conjugated goat anti-rabbit IgG (Zhongshan Biotechnique, Beijing, China) as the secondary antibody.

2.7. In vitro enzymatic reaction for detection of DXP and MEP

The DXS assay uses 1 ml of reaction mixture containing 110 mM fructose-1,6-diphosphate (pH 7.5), 10 mM $MgCl_2$, 120 mM Tris-HCl (pH 7.5), 60 U aldolase, 60 U triose phosphate isomerase, and 5 mM β-mercaptoethanol. This solution was heated in a water bath at 25 °C for 1 h. After the reaction, the substrates of DXS, dihydroxyacetone phosphate and glyceraldehyde-3-phosphate, were obtained. Then, 2 ml of reaction mixture was performed to identify the enzymatic reaction for detection of DXP, which contained 110 mM sodium pyruvate, 2 mM TPP, and 100 μg DXS, 100 mM Tris-HCl (pH 7.5). The final volume (2.0 ml) of reaction mixture was adjusted by adding water, and the mixture solution was incubated at 37 °C for 16 h. After completion of the reaction, the solution was passed through a 10-kD filter by centrifugation at 11,000 rpm for 10 min and immediately freeze-dried. For the DXR assay, 1 ml of reaction mixture was used, which contained 100 mM Tris-HCl (pH 7.5), 2 mM $MgCl_2$, 0.12 mM NADPH, the powder described above, 200 μg DXR, and H_2O to a final volume of 1 ml. This solution was heated in a water bath at 37 °C for 12 h, and the reaction was terminated by incubation at 100 °C for 10 min. The solution was then passed through a 10-kD filter by centrifugation at 11,000 rpm for 10 min and immediately freeze-dried. *E. coli* BL21 (DE3) carrying an empty vector treated with the same conditions was used as a negative control.

Quantitative analysis of PtDXS and PtDXR reaction products was performed by high-performance liquid chromatography (HPLC)/mass spectrometry (MS) using the Agilent poroshell 120 SB-C18 reversed-phase column. The column temperature was set to 30 °C. The mobile phase contained 80% methanol and 20% water (0.1% formic acid) and was eluted using a gradient of 200 μL/min. The MS conditions were as follows: spray voltage of 4000 V (+)/3500 V (−), air curtain of 15 psi, atomizing gas pressure of 45 psi, auxiliary pressure of 60 psi, and atomization temperature of 340 °C. Standard products were identified by mass spectra with fragment ions; 213/79.0 fragment ions were chosen as the qualitative ions for DXP, and 215/79.0 fragment ions were chosen as the qualitative ions for MEP. Moreover, the calibration curves for DXP and MEP are shown in Fig. S1, and the reactions for standard products containing DXP and MEP are shown in Fig. S2.

2.8. Transcription of PtDXS and PtDXR in various tissues

Total RNA was isolated from mature and young leaves, upper and lower stems, petioles, and roots of *P. trichocarpa*. Quantitative reverse transcription PCR (qRT-PCR) was performed using the conditions described above. qRT-PCR primers were designed for PtDXS and PtDXR (Table 1), and the housekeeping gene actin was used as an internal control. qRT-PCR was performed as follows: initial incubation at 95 °C for 5 min, followed by 40 cycles of 45 s at 95 °C, 45 s at the annealing temperature at 60 °C, and 45 s at 72 °C, and a final incubation for 10 min at 72 °C. Triplicate measurements were performed for each of these parameters, and each data point represents a mean value. The treatments were repeated three times for analyses of PtDXS and PtDXR transcription in various tissues.

2.9. Expression of PtDXS and PtDXR in different stress treatment

Poplar seedlings were first placed in half-strength Murashige and Skoog (Murashige et al., 2010) medium for 1 week and then removed and placed in medium containing 200 mM NaCl, 200 μM abscisic acid (ABA), and 2 mM hydrogen peroxide (H_2O_2). *P. trichocarpa* seedlings treated with 200 mM NaCl, 200 μM ABA, and 2 mM H_2O_2 were sampled at 0, 2, 4, 6, 8, 12, 24, and 48 h, and those subjected to 4 °C cold stress and 10% PEG_{6000} were collected after 1, 2, 3, 4, 5, 6, and 7 days. Subsequently, qRT-PCR was performed as described above. Triplicate measurements were performed for each parameter, and each data point represents a mean value. The treatments were repeated three times for analyses of PtDXS and PtDXR expression in response to abiotic stress treatment.

Table 1
Sequence information for PtDXS and PtDXS.

Gene name	Full length (bp)	ORF (bp)	Amino acid sequence (aa)	Molecular weight (kDa)	PI
PtDXS	2567	2166	721	77.733	6.72
PtDXR	2296	1416	471	51.214	5.77

2.10. Expression profiles of PtDXS and PtDXR transcripts at different times

Leaves of 3-month-old *P. trichocarpa* were extracted on two consecutive days, July 27 and July 28, 2016 at 4-h intervals over the course of 48 h. The collected leaves are immediately frozen in liquid nitrogen, and RNA was immediately extracted from the leaves and qRT-PCR was performed as described above. Triplicate measurements were performed for each of these parameters, and each data point represents a mean value. The treatments were repeated three times for analyses of *PtDXS* and *PtDXR* transcript expression profiles at different times.

2.11. Construction of the vector pGWB9-PtDXR and detection of transgenic poplars

We used two-step method to construct overexpression vector. Firstly, the ORF of *PtDXR* gene was cloned into vector pDONRTM/Zeo based on the BP reaction. Secondly, the fused pDONRTM/Zeo-*PtDXR* was a template, and the ORF of *PtDXR* gene was cloned into vector pGWB9. Finally, the fused plasmid pGWB9-*PtDXR* was introduced into *Agrobacterium tumefaciens* strain EHA105 (maintained in our laboratory).

Young leaves and petioles of the Nanlin895 poplar were prepared by pre-culturing for 3 days on differentiation Murashige and Skoog medium (MS medium supplemented with 0.5 mg/L 6-BA and 0.002 mg/L TDZ). *Agrobacterium tumefaciens* strain EHA105 carrying the *DXR* gene was used to infect plants when the agrobacterial concentration reached OD 0.6 at 600 nm. Subsequently, the potential resistant strains were screened for differentiation medium (MS medium supplemented with 0.5 mg/L 6-BA and 0.002 mg L TDZ, 30 mg/Lkanamycin), bud elongation medium (MS medium supplemented with 0.25 mg/L 6-BA, 0.002 mg/L TDZ, and 15 mg/L kanamycin) and rooting medium (1/2 MS medium supplemented with 10 mg/L kanamycin) respectively. The putative transgenic lines were selected by using PCR. Regenerated shoots from the putative transgenic lines were recovered and transferred to half-strength Murashige and Skoog rooting medium supplemented with 10 mg/L kanamycin.

2.12. Transplantation of wild-type poplars and transgenic lines

The wild-type poplars and transgenic lines grown on half-strength MS rooting medium for 4 weeks were moved to a greenhouse. Firstly, closures were removed and wild-type poplars and transgenic lines undergo three days of environmental adaptation. Secondly, the wild-type poplars and transgenic lines were transplanted into mixed soil (sterilized peat and perlite 2:1), and vinyl membranes were covered the surface of the flowerpot. After a period of growth, the vinyl membranes were removed and we water the plants every day.

2.13. Salt and drought treatments

For analysis of salt- and drought-stress, 4-month-old Nanlin895 plants grown in a greenhouse were used. For salt stress treatment, WT plants and nine transgenic lines were irrigated with 1 L of 200 mM NaCl solution every day for 2 weeks. For drought stress treatment, the water

supply was shut off for 2 weeks. In addition, A microplate reader (Bio-Rad, Hercules, CA, USA) was used to determine the proline (Pro), superoxide dismutase (SOD), and peroxidase (POD) activities, as well as the malondialdehyde (MDA) level. The salt and drought treatments were repeated at least three times.

2.14. Relative water content (RWC) analysis of WT and transgenic poplars under drought and salt stresses

RWC was measured as described previously (Li et al., 2011) with the following formula: RWC (%) = [(FW – DW)/(TW – DW)] × 100, where FW = fresh weight of newly collected leaves (measured immediately after collection), TW = turgid weight of leaves after incubation in water for 6 h at 20 °C in the light, and DW = dry weight of the same leaves after drying at 80 °C for 48 h. RWC was measured in the first fully expanded leaf from the top. Triplicate measurements were performed for each of these parameters, and each data point represents a mean value. The treatments were repeated three times for RWC analyses in WT and transgenic poplars under drought and salt stresses.

2.15. Pathogen inoculation treatment and disease response assay

For the *S. populiperda* infection assay, pathogens were grown at 23 °C on potato dextrose agar (PDA) medium for 1 week. Leaves from the same position on 4-month-old transgenic and WT poplars were punctured with a 5-ml syringe needle and inoculated with a small amount of PDA containing the pathogen or the same amount of PDA as a negative control. Pathogenic soft rot symptoms were evaluated periodically. The maximal lesion sizes (diameter; mm) on leaves were recorded at 24 and 48 h as previously described (Li et al., 2011) Moreover, microscopic observation was used to detect the time of conidia appearance in WT and transgenic poplars. Each experiment was repeated at least three times.

2.16. Sequence analysis

Gene sequences were archived online (http://www.ncbi.nlm.nih.gov/; https://phytozome.jpi.doe.gov/pz/portal.html). Nucleotide sequences, deduced amino acid sequences, and ORFs of DXS and DXR were analyzed using ExPASy online (http://www.expasy.org/translate/). Computed Pi/Mw values from ExPASy online (http://www.expasy.org/tools/pi_tool.html) were used to calculate molecular weights (MWs) and predict isoelectric points (pIs). The Scanprosite search function of the PROSITE database was used in ExPASy online (http://www.expasy.org/prosite/) to analyze the structural and functional domains. The PORTER server at Dublin University (http://distil.ucd.ie/porter/) was used to predict secondary structures. The SWISS-MODEL server (http://www.expasy.org/swissmod/SWISS-MODEL.html) was used to predict tertiary structures. A multiple alignment analysis of the amino acid sequences of *PtDXS* and *PtDXR* was carried out using MEGA software.

3. Results

3.1. Molecular cloning and sequences analysis of PtDXS and PtDXR

In this study, the full-length cDNAs of DXS and DXR were isolated from *P. trichocarpa*, termed *PtDXS* (Potri.010G015200.1) and *PtDXR* (XM_OO2318012.2). The *PtDXS* ORF is 2166 base pairs (bp) in length and encodes a peptide of 721 amino acids, while the *PtDXR* ORF is 1416 bp and encodes a peptide of 471 amino acids. According to the *PtDXS* and *PtDXR* sequences, we designed special primers and achieved full-length amplification of *PtDXS* and *PtDXR* using RACE. The full lengths of the genes, ORF sizes, the lengths of amino acid sequences, MWs, and pIs of each deduced protein are shown in Table 1. The deduced amino acid sequence of PtDXS showed a high degree of homology with DXS sequences from other plant species, e.g., *Theobroma cacao* (XP_017975597.1, 85.33% identity), *Prunus persica* (XP_007225144.1, 85.08% identity), *Bixa orellana* (AMJ39459, 84.89% identity), and *M. truncatula* (CAD22530.1, 80.78% identity) (Fig. S3A) (Fig. S2). PtDXR had 87.25, 85.42, 84.88, and 80.04% identity with DXRs from *Hevea brasiliensis* (ABD92702.1), *Rosa rugosa* (AEZ53171.1), *Tripterygium wilfordii* (AHW46302.1), and *A. thaliana* (AED97657.1) (Fig. S3B).

3.2. Bioinformatics analysis

Plant DXSs and DXSs contain a chloroplast (plastid) transit peptide, directing the enzyme to plastids in which the MEP pathway is located. For PtDXS, a conserved cleavage site of an NADH-binding motif (Khemvong and Suvachittanont, 2005) is located at the C-terminus of PtDXS. PtDXS contains a TPP-binding domain (Xiang et al., 2007) at the N-terminus, which may contribute to the catalytic activity of DXS (Fig. S3A). A putative conserved cleavage site in the DXR motif (Carretero-Paulet et al., 2002; Hans et al., 2004) is located at the N-terminus of PtDXR, and the NADPH-binding (Lange et al., 1998) domains are involved in the transformation of DXP to MEP (Fig. S3B). The predicted tertiary structures of PtDXS and PtDXR are shown in Fig. S3C and D.

3.3. Prokaryotic expression, purification, and Western blot

According to restriction site analysis, the ORF of the *PtDXS* gene of *P. trichocarpa* was inserted into vector PET-28a between the NotI and *Bam*HI restriction sites (Fig. S4A) and the ORF of the *PtDXR* gene was inserted into vector PET-28a between the NcoI and *Bam*HI restriction sites (Fig. S4B). We verified the recombinant prokaryotic expression vectors (PET-28a-PtDXS and PET-28a-PtDXR) by sequencing. IPTG-induced bacteria were analyzed using 12% SDS-PAGE. The results for PtDXS showed a specific band of the expected size of 78.4 kDa (Fig. 1A), and a specific band of the expected size of 51.8 kDa was identified for PtDXR, both of which include the 6*His-tag (Fig. 1B). In addition, according to the results of precipitation and supernatant, we determined that the expressed proteins existed as inclusion bodies. The two pure target proteins were performed by the techniques of refolding and re-

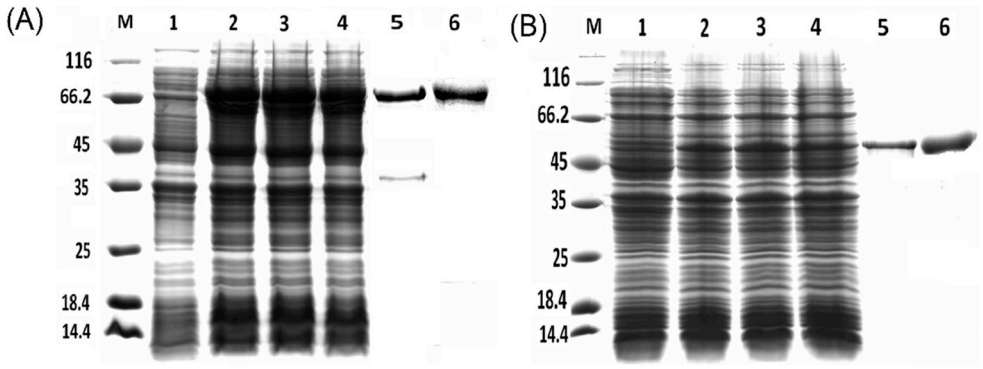

Fig. 1. (A) Analysis of expressed fusion proteins containing *PtDXS* via 12% sodium dodecyl sulfate polyacrylamide gel electrophoresis (SDS-PAGE). M: protein marker; 1: uninduced; 2–4: induced with 1 mM isopropyl β-D-1-thiogalactopyranoside (IPTG); 5: purified PtDXS; 6: Western blot of PtDXS protein. (B) Analysis of expressed fusion proteins containing *PtDXR* by 12% sodium dodecyl sulfate polyacrylamide gel electrophoresis (SDS-PAGE). M: protein marker; 1: uninduced; 2–4: induction with 1 mM IPTG; 5: purified PtDXR; 6: Western blot of PtDXR protein.

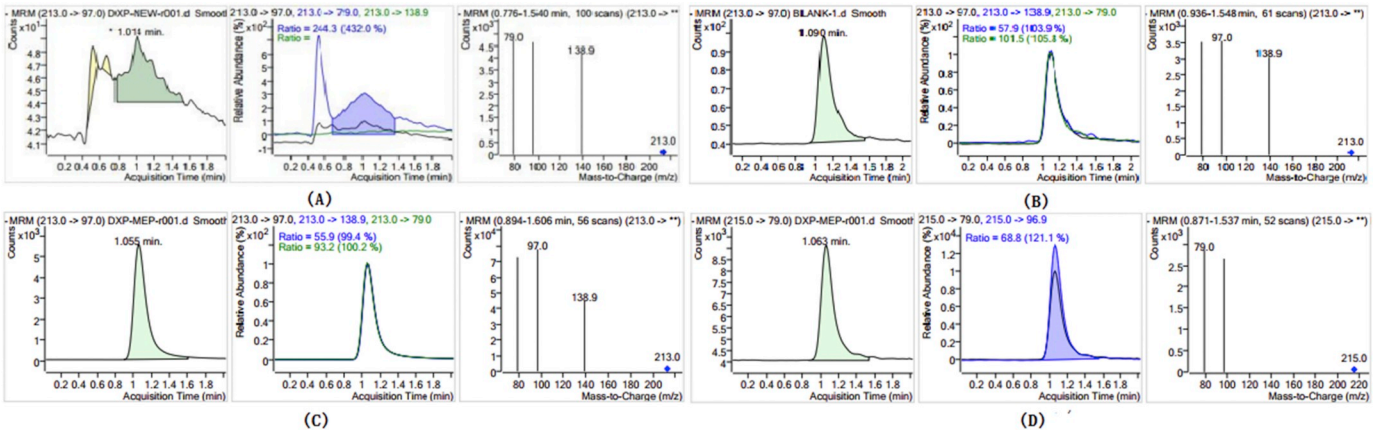

Fig. 2. All reaction products of high performance liquid chromatography tandem mass spectrometry (HPLC–MS/MS) analysis of 1-deoxy-D-xylulose 5-phosphate (DXP) and 2-C-methyl-D-erythritol 4-phosphate (MEP). (A, B) All reaction products from HPLC–MS/MS analysis of DXP (negative control group [A] and sample group [B]). (C, D) All reaction products from HPLC–MS/MS analysis of MEP (negative control group [C] and sample group [D]). For DXP, a total of 2 fragment ions, 213/138.9 and 213/79.0, were detected by DXP. 213/138.9 was used as the quantitative ion. DXP were quantified by the ion detection response. 213/79.0 fragment ions are DXP qualitative ions. The qualitative ion of 213/79.0 fragment was appeared. For MEP, a total of 2 fragment ions, 215/96.9215/79.0, were detected by MEP. 215/96.9 was used as the quantitative ion.

dissolving (Fig. 1A and B). Western blotting analysis was used to determine whether PtDXS and PtDXR could be specifically recognized by rabbit antiserum against His-DXS and His-DXR expressed in *E. coli* BL21 (DE3). The results indicated that the rabbit antiserum successfully identified His-DXS and His-DXR, confirming that the BL21 (DE3)-expressed peptides were DXS and DXR (Fig. 1A and B).

3.4. Functional identification of PtDXS and PtDXR

To confirm that whether PtDXS and PtDXR are functional genes, the HPLC/tandem MS (HPLC–MS/MS) was used to determine the reaction of purified enzymes preliminary. 2 fragment ions, 213/138.9 and 213/79.0, were detected by DXP. 213/138.9 was used as the quantitative ion. DXP were quantified by the ion detection response. 213/79.0 fragment ions are DXP qualitative ions. In Fig. 2B, the qualitative ion of 213/79.0 fragment was appeared, so DXP was generated. However, for Fig. 3A, the qualitative ion of 213/79.0 fragment was not appeared. 2 fragment ions, 215/96.9215/79.0, were detected by MEP. 215/96.9 was used as the quantitative ion. MEP was quantified by the ion detection response. For Fig. 2D, the qualitative ion of 215/79.0 fragment was appeared, so MEP was generated. For Fig. 2C, we did not identified mass spectra 215/79.0 fragment ions, only the qualitative ion of 213/79.0 fragment for DXP. Comparison of the retention times and mass fragmentation patterns of samples with DXP and MEP standards (Sigma, St. Louis, MO, USA) confirmed that the recombinant PtDXS and PtDXR enzymes were active and formed the downstream products of DXP (Fig. 2B) and MEP (Fig. 2D). In contrast, no peaks or mass fragmentation patterns were detected in the control, which did not contain enzyme in the reaction mixture (Fig. 2A and C).

3.5. Analysis of tissue-specific expression of PtDXS and PtDXR

qRT-PCR was employed to investigate the expression of PtDXS and PtDXR in different tissues (mature and young leaves, upper and lower

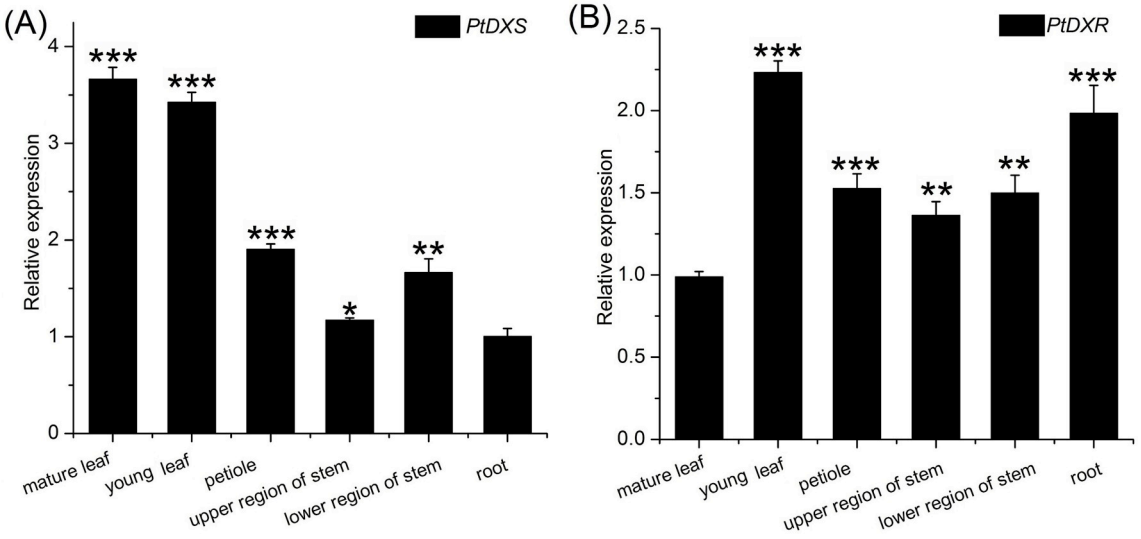

Fig. 3. Expression analysis of the *PtDXS* and *PtDXR* genes in various tissues. Mean levels (with standard deviations [SD]) in six tissues were analyzed using real-time quantitative polymerase chain reaction (qPCR). Data presented are $2^{-\Delta\Delta Ct}$ levels calculated relative to the special tissue (root), which was set to 1, and normalized to mRNA levels of actin. Three independent experiments were performed. Vertical bars represent means ± SD (n = 3). Asterisk indicates a significant difference at $P < 0.05$. Double asterisk indicates a significant difference at $P < 0.01$.

stems, petioles, and roots). The expression patterns showed that both PtDXS and PtDXR were expressed extensively in all examined tissues. PtDXS showed the highest expression level in young leaves and the lowest expression level in roots, with expression in the young leaves almost 3.7-fold higher than that in the roots (Fig. 3A). All of these results for PtDXS are similar to findings in other species, including *A. thaliana* (Estevez et al., 2001), *T. wilfordii* (Tong et al., 2015), *Amomum villosum* (Yang et al., 2012), and *Aquilaria sinensis* (Xu et al., 2014). Previous research has shown that type I DXS exists in most plant tissues and participates in primary metabolism (Cordoba et al., 2011). PtDXR, which is expressed at the highest levels in young leaves, had its highest levels in roots and petioles, followed by the upper stems and lower stems, and is lowest in the mature leaves (Fig. 3B). However, the differences in the transcript levels of PtDXR were relatively small; in particular, the differences between the petioles and upper and lower stems were small. These results indicated that these two genes follow a tissue specific pattern.

3.6. Transcript level of PtDXS and PtDXR following induction with 200 mM NaCl, 200 μM ABA, 2 mM H_2O_2, 4 °C cold stress, and 10% PEG_{6000}

To characterize the transcription pattern of PtDXS and PtDXR under stress, we subjected seedlings of *P. trichocarpa* to the following abiotic stresses: 200 mM NaCl, 200 μM ABA, 2 mM H_2O_2, 4 °C cold stress, and 10% PEG_{6000}. The results revealed that the transcription levels of PtDXS and PtDXR were altered in response to the treatments to varying degrees. The highest level of PtDXS expression was observed at 12 h of 200 μM ABA treatment, with an expression approximately 2.3 times that of the control, which was followed by a gradual decline (Fig. 4A). Following treatment with 10% PEG_{6000} for 7 days, PtDXS transcription was upregulated approximately 4-fold (Fig. 4C). The expression of PtDXS was enhanced at 3–48 h of 200 mM NaCl treatment, and was only reduced at 1 h (Fig. 4B). Following treatment with the abiotic stress 2 mM H_2O_2, the expression of PtDXS declined during the first 6 h and was subsequently upregulated, reaching a level approximately 2. fold higher than the control at 24 h (Fig. 4E). PtDXS expression was strongly induced by 4 °C cold stress (control temperature, 23 °C) and reached a maximum level of expression after 7 days of treatment (Fig. 4D).

As shown in Fig. 5, PtDXR expression was increased under the abiotic stress treatments. Treatment with 100 mM ABA for 12 h resulted in a transcript level of PtDXR approximately 20-fold greater than the control level (Fig. 5A). Following treatment with 10% PEG_{6000}, the highest expression of PtDXR was evident on day 5 (Fig. 5C), while with 4 °C cold stress, expression levels were approximately 30-fold above the control levels (Fig. 5D). The expression of PtDXR declined during the first 3 h and then increased, reaching the highest level at 24 h of 2 mM H_2O_2 treatment (Fig. 5E). For the abiotic stresses, 200 mM NaCl showed the greatest effect, with an approximately 60-fold increase in PtDXR expression at 48 h (Fig. 5B). In addition, the expression peaks of PtDXR induced by abiotic stress treatments were higher than those of PtDXR induced by abiotic stress treatments (Fig. 5). These data suggest that PtDXS and PtDXR may play roles in the response pathways induced by abiotic stress in poplar and that PtDXR has a more significant role under abiotic stress.

3.7. Expression profiles of PtDXS and PtDXR transcripts at different times

Leaves of 3-month-old *P. trichocarpa* plants were extracted at 4-h intervals over the course of 48 h on two consecutive days, July 27 and July 28, 2016. The transcript level of PtDXS in leaves exhibited diurnal changes. The expression of the *PtDXS* gene was higher during conditions of light compared with the dark (Fig. 6A). The expression pattern of PtDXS was similar to that observed in previous studies of gray poplar leaves (Loivamaki et al., 2007). On the other hand, no diurnal variation was observed for PtDXR (Fig. 6B).

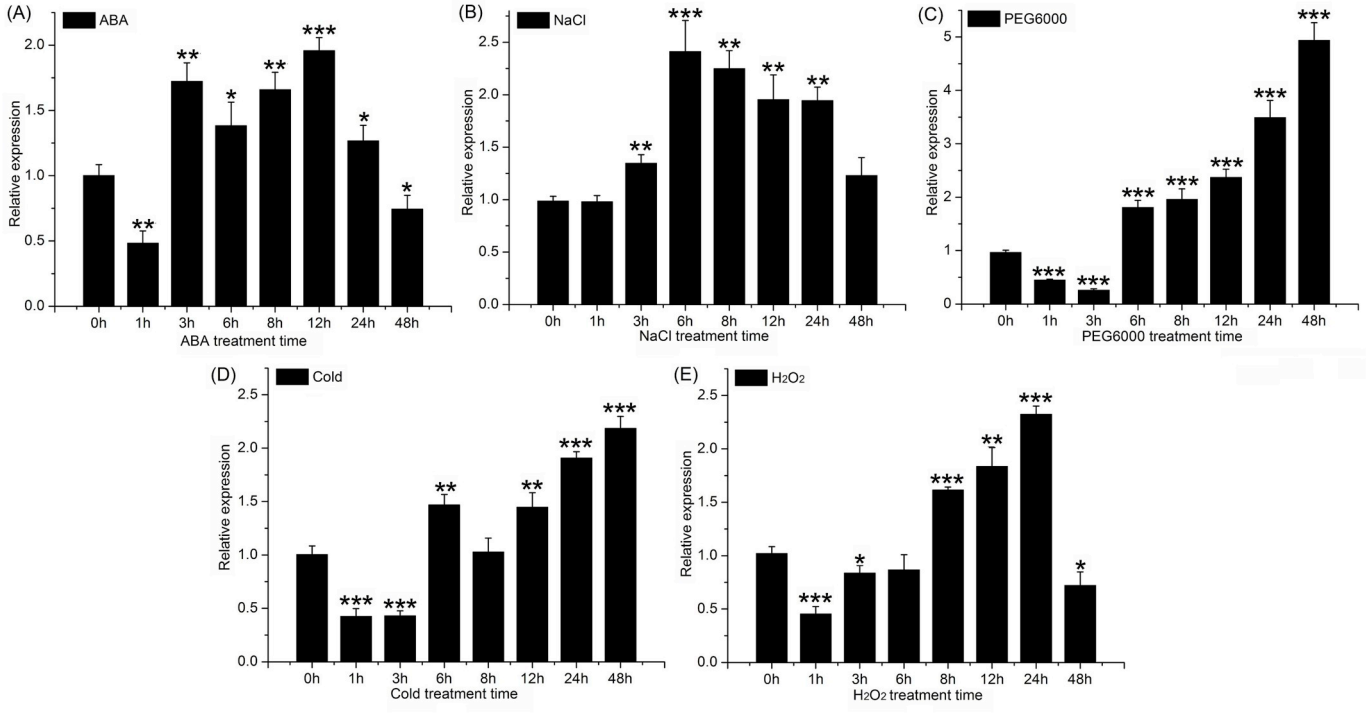

Fig. 4. Expression time-course of *PtDXS* in response to different stress treatments, as determined by qPCR. qPCR was performed with total RNA extracted from leaves at the indicated times after treatment with 200 μM abscisic acid (ABA) (A), 200 mM NaCl (B), 10% PEG_{6000} (C), 4 °C (D), and 2 mM hydrogen peroxide (H_2O_2) (E). Relative expression was calculated using actin as an internal reference. Leaves treated with distilled water under the same conditions served as controls. Vertical bars represent means ± SD (n = 3). Three independent experiments were performed. Asterisk indicates a significant difference at $P < 0.05$. Double asterisk indicates a significant difference at $P < 0.01$.

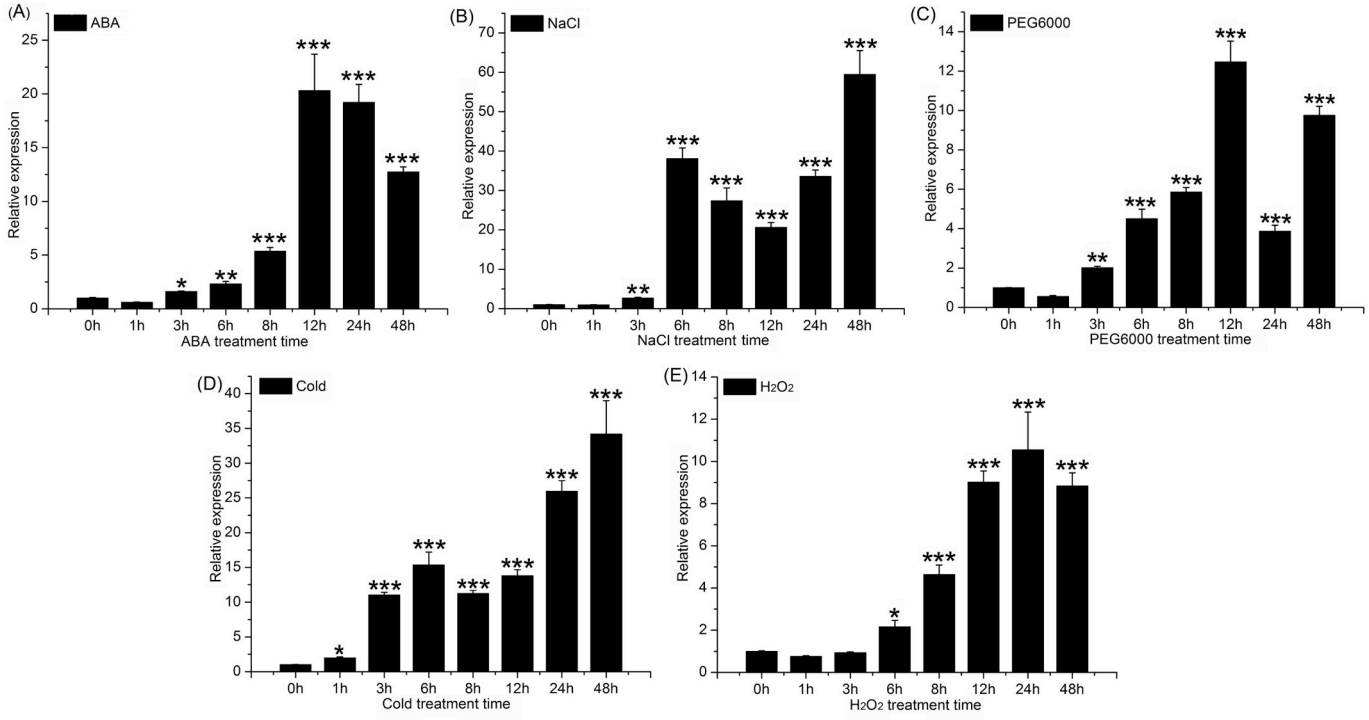

Fig. 5. Expression time-course of *PtDXR* in response to different stress treatments, as determined by qPCR. qPCR was performed with total RNA extracted from leaves at the indicated times after treatment with 200 μM ABA (A), 200 mM NaCl (B), 10% PEG_{6000} (C), 4 °C (D), and 2 mM H_2O_2 (E). Relative expression was calculated using actin as an internal reference. Leaves treated with distilled water under the same conditions served as controls. Three independent experiments were performed. Vertical bars represent means ± SD (n = 3). Asterisk indicates a significant difference at $P < 0.05$. Double asterisk indicates a significant difference at $P < 0.01$.

3.8. Expression of PtDXR in the Nanlin895 poplar

The putative transformants regenerated on selective Murashige and Skoog medium were transferred to MS medium supplemented with additional hormones for shoot formation, then to half-strength MS medium for rooting. Finally, well-developed poplar plants were transplanted into the greenhouse. We performed an initial screening of putative transgenic Nanlin895 poplars through PCR analysis of genomic DNA using PtDXR-specific primers (Table S1). Eight transgenic lines were selected for qRT-PCR analysis, and the result showed that the *PtDXR* gene can be expressed stably in Nanlin895 poplars (Fig. 7A). Total proteins from both WT and transgenic poplars were extracted and analyzed by 12% SDS-PAGE (Fig. 7B). Western blotting was used to determine whether PtDXR could be specifically recognized by rabbit antiserum against His-DXR expressed in transgenic poplars. The results showed that the antibody successfully identified His-DXR, confirming that the transgenic poplar-expressed peptides were DXR (Fig. 7C). Western blotting also revealed that the *PtDXR* gene was stably integrated into the genomes of the R1-1, R2-4, R3-1, R4-7, R5-3, R6-1, R7-3, and R8-2 lines and led to expression of the DXR protein using the expression system of the poplar. Based on the qRT-PCR and western blotting results, transgenic lines R1-1, R2-4, R3-1, R4-7, R5-3, R6-1, R7-3, and R8-2 were selected for further study.

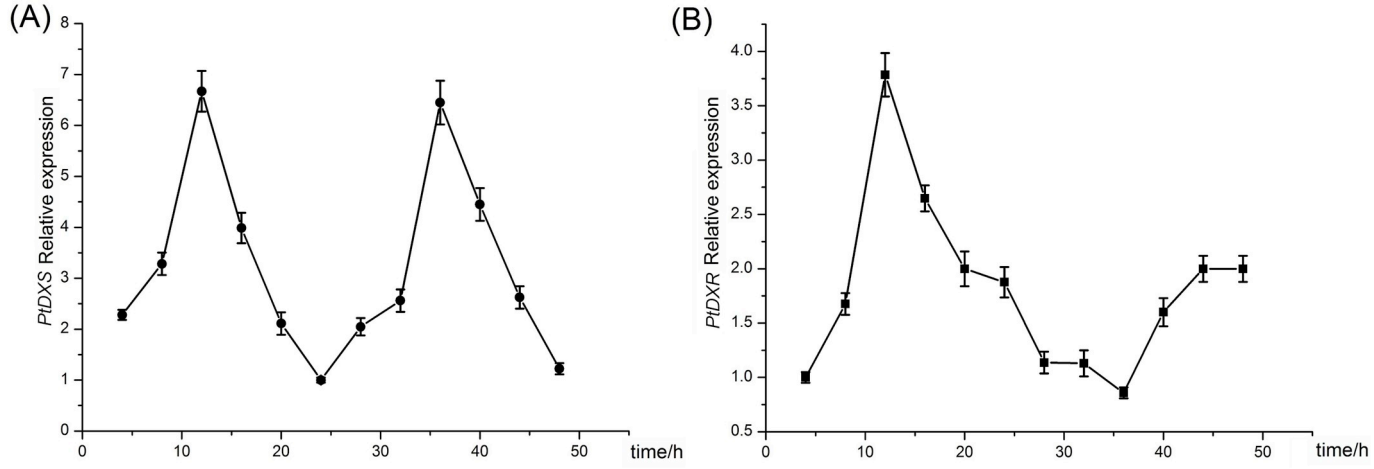

Fig. 6. Diurnal variation analysis of *PtDXS* and *PtDXR*. (A, B) Expression profiles of *PtDXS* (A) and *PtDXR* (B) at different times from leaves extracted at 4-h intervals over the course of 48 h on July 27 and July 28, 2016. Three independent experiments were performed.

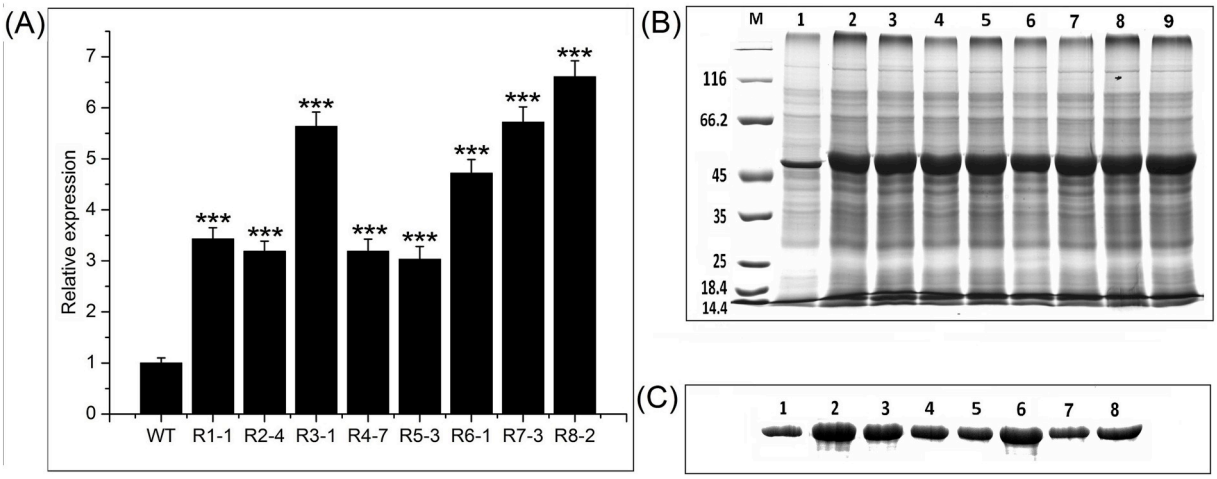

Fig. 7. Molecular identification of regenerated *PtDXR* transgenic poplar plants. (A) Quantitative reverse transcription PCR analysis of transcript levels of *DXR* in wild-type (WT) plants and plants overexpressing *PtDXR*. (B) SDS-PAGE analysis of total protein from WT and transgenic poplar plants. M: protein marker; 1–9: protein expression levels of WT, R1-1, R2-4, R3-1, R4-7, R5-3, R6-1, R7-3, and R8-2 plants, respectively. (C) Western blot of PtDXR protein using a monoclonal antibody against the 6*His tag. 1–8: proteins from R1-1, R2-4, R3-1, R4-7, R5-3, R6-1, R7-3, and R8-2 plants, respectively.

3.9. Statistics of poplar growth

We transferred similarly sized WT and transgenic poplars that had been rooted on half-strength MS medium to pots filled with equal quantities of mixed soil including sterilized peat and perlite (7:2:1) in a greenhouse to compare plant growth among the different lines. The shoot heights and showed marked differences after 2 and 4 months of growth in the greenhouse (Fig. S5). Poplar phenotypic growth indicators included shoot height, stem diameter, number of leaves, the result showed that those phenotypic growth indicators in transgenic lines exhibited significantly greater that in wild-type poplars (Table 2).

3.10. Evaluation of salt and drought tolerance in poplar plants in a greenhouse

Salt and drought stresses were used to evaluate the tolerances of the transgenic lines and WT plants after 4 months of growth in a greenhouse. Drought stress was achieved by withholding water for 2 weeks. Salt stress was evaluated by irrigating the plants with a solution of 200 mM NaCl for 2 weeks. Under normal conditions, transgenic plants were taller than WT plants (Fig. S6A and B). After 2 weeks of drought treatment, the eight transgenic lines continued to grow well, and exhibited higher rates of greening than the WT plants. Only some lower leaves of the transgenic plants turned yellow, whereas the growth of WT plants was significantly inhibited (Fig. S6B). For the detection of relative water content, the result showed that water content in leaves of transgenic plants was significantly higher than that in leaves of wild

Table 2
Comparison of growth between transgenic and wild-type (WT) poplars.

No. of poplar	Culture period	Shoot height (cm)	Stem diameter (mm)	No. of leaves	Length of largest leaf (cm)	Width of largest leaf (cm)
WT	1 week	4.77 ± 0.25	1.35 ± 0.03	5	1.77 ± 0.09	1.39 ± 0.09
	2 months	15.33 ± 0.31	3.07 ± 0.03	10	3.69 ± 0.07	2.75 ± 0.17
	4 months	29.73 ± 0.64	3.45 ± 0.06	13	4.24 ± 0.14	3.19 ± 0.15
R1-1	1 week	4.77 ± 0.25	1.37 ± 0.04	7	1.72 ± 0.07	1.51 ± 0.08
	2 months	22.87 ± 0.81	3.54 ± 0.07	17	6.16 ± 0.12	4.84 ± 0.26
	4 months	47.67 ± 2.89	4.13 ± 0.1	20	9.44 ± 0.21	7.62 ± 0.26
R2-4	1 week	4.83 ± 0.21	1.37 ± 0.06	6	1.87 ± 0.09	1.45 ± 0.10
	2 months	24.2 ± 1.02	3.49 ± 0.09	17	6.6 ± 0.09	5.34 ± 0.19
	4 months	49.33 ± 3.01	4.04 ± 0.08	19	9.31 ± 0.12	7.7 ± 0.18
R3-1	1 week	4.97 ± 0.15	1.38 ± 0.04	6	1.83 ± 0.11	1.54 ± 0.12
	2 months	23.1 ± 1.01	3.52 ± 0.11	16	6.26 ± 0.12	4.50 ± 0.17
	4 months	49.33 ± 1.15	4.06 ± 0.14	19	9.47 ± 0.19	7.19 ± 0.23
R4-7	1 week	5.03 ± 0.15	1.4 ± 0.06	7	1.82 ± 0.10	1.47 ± 0.09
	2 months	25.13 ± 1.06	3.54 ± 0.08	19	7.23 ± 0.17	5.24 ± 0.11
	4 months	59.33 ± 4.04	4.16 ± 0.18	23	9.97 ± 0.26	8.52 ± 0.37
R5-3	1 week	4.99 ± 0.12	1.37 ± 0.07	5	1.78 ± 0.08	1.42 ± 0.07
	2 months	22.93 ± 0.74	3.53 ± 0.10	16	6.86 ± 0.62	5.48 ± 0.33
	4 months	50.40 ± 0.80	4.13 ± 0.09	19	9.79 ± 0.50	7.35 ± 0.34
R6-1	1 week	4.97 ± 0.14	1.36 ± 0.05	6	1.81 ± 0.11	1.52 ± 0.15
	2 months	23.15 ± 0.56	3.53 ± 0.07	17	6.74 ± 0.12	5.34 ± 0.17
	4 months	50.62 ± 1.43	4.19 ± 0.09	20	972 ± 0.41	7.69 ± 0.26
R7-3	1 week	5.01 ± 0.08	1.4 ± 0.07	7	1.78 ± 0.13	1.45 ± 0.09
	2 months	24.8 ± 0.63	3.58 ± 0.05	19	6.76 ± 0.22	5.28 ± 0.14
	4 months	55.15 ± 1.92	4.21 ± 0.17	22	10.03 ± 0.25	8.35 ± 0.41
R8-2	1 week	4.97 ± 0.11	1.38 ± 0.09	7	1.83 ± 0.12	1.43 ± 0.12
	2 months	24.37 ± 1.20	3.51 ± 0.11	19	6.88 ± 0.29	5.48 ± 0.12
	4 months	52.62 ± 0.88	4.14 ± 0.14	22	10.05 ± 0.31	7.90 ± 0.22

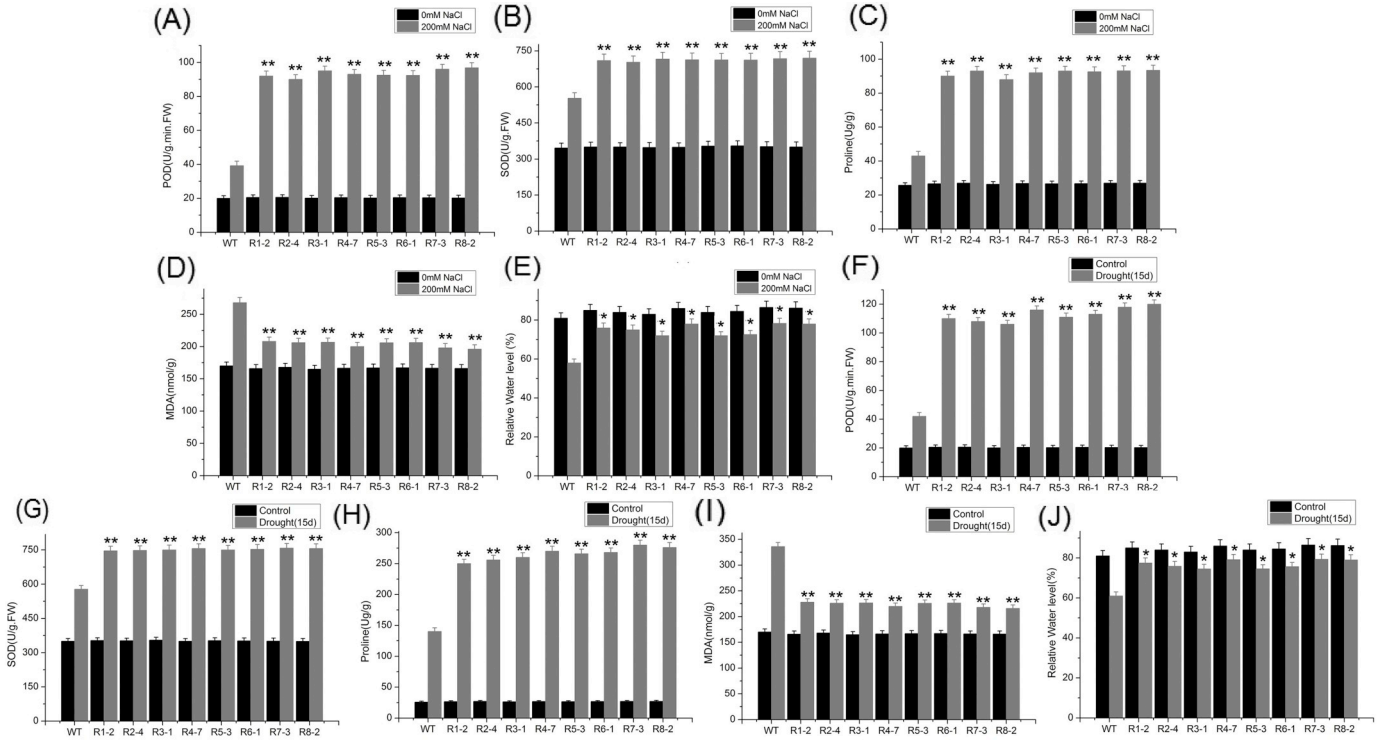

Fig. 8. Phenotypic analysis of WT and *PtDXR* transgenic plants before and after drought and salt treatments. (A) Guaiacol peroxidase activity under salt stress. (B) Superoxide dismutase (SOD) activity under drought treatment. (C) Free proline (Pro) content under drought treatment. (D) Malondialdehyde (MDA) activity under drought treatment. (E) Relative water content (RWC) after 2 weeks of water-withholding drought treatment. (F) Guaiacol peroxidase activity under salt stress. (G) SOD activity under salt stress. (H) Free Pro content under salt stress. (I) MDA activity under salt stress. (J) RWC after 2 weeks of water withholding under salt stress. Three independent experiments were performed. Vertical bars represent means ± SD (n = 3). Asterisk indicates a significant difference at $P < 0.05$. Double asterisk indicates a significant difference at $P < 0.01$.

type poplar (Fig. 8E). For the Pro content, the Pro content in transgenic plants improved significantly than that WT plants under the drought treatment (Fig. 8C). In addition, we also analyzed the SOD and POD activities before and after drought treatment, and the results shower that SOD and POD activities were increased significantly in the transgenic plants when compared with that in WT plants. However, by comparing the transgenic and WT plants under drought stress, we observed significant differences in both POD and SOD activities (Fig. 8A and B). Under normal conditions, a lower MDA level was observed in the transgenic lines compared with WT plants, and levels decreased by an average of 1.6-fold in the WT and transgenic lines subjected to drought stress for 2 weeks (Fig. 8D).

To determine whether the overexpression of PtDXR increases plant tolerance to salt stress, the phenotype, RWC, SOD and POD activities, MDA level, and Pro content of each plant under salt stress were analyzed. After 2 weeks of salt-stress treatment, growth of the WT plants was significantly inhibited compared with the transgenic lines (Fig. S6). The transgenic lines continued to grow well and exhibited only slight yellowing of a few leaves, whereas the growth of WT plants was significantly inhibited (Fig. S6A and C). As shown in Fig. 8F and G, the transgenic lines had slightly higher SOD and POD activities than WT under normal conditions. Under drought and salt stresses, the SOD and POD activities were 1.55-fold and 2.25-fold higher, respectively, in all transgenic lines compared with WT plants. Pro is an important osmoprotectant, which protects cells from damage under salt stress. As shown in Fig. 8H, Pro content was significantly higher in transgenic lines than WT under salt stress. Under normal conditions, the RWC of the transgenic lines did not differ significantly from WT (Fig. 8J). However, when treated with salt stress, transgenic lines and WT plants exhibited decreased RWC, and the dampness of the transgenic lines was significantly lower than that of WT. Moreover, MDA levels in transgenic lines was lower than that in WT plants, and MDA levels under normal conditions, and MDA levels were decreased by 26% in transgenic lines and WT plants under drought stress (Fig. 8I).

3.11. Transcript levels of PtDXR increase in response to S. populiperda infection

To evaluate whether the *PtDXR* gene is involved in defense against *S. populiperda*, time-course and necrotic symptom studies were conducted with both transgenic lines and WT Nanlin895 poplars infected with *S. populiperda*. The appearance of conidia occurred in WT plants 2 days after inoculation, whereas the transgenic lines only began to exhibit conidia after 4 days (Fig. 9). Moreover, the spread and extent of pathogens in the WT plants were faster and greater than in the transgenic lines, based on analysis of the length and width of the largest pathogenic region (Fig. 10). Time-course and necrotic symptom studies of leaves revealed that PtDXR-overexpressing lines exhibited higher resistance to pathogens than WT plants.

4. Discussion

In plants, there are at least two distinct pathways that generate isoprenoid precursors: the MEP and MVA pathways (Lichtenthaler, 1999; Rohmer, 1999; Eisenreich, 2001; Shen et al., 2006). Two enzymes in the MEP pathway, DXS and DXR, catalyze the first and second major steps. Therefore, DXS and DXR are considered the most important rate-limiting enzymes of the MEP pathway. In this study, we obtained full-length cDNAs of PtDXS and PtDXR and found that the predicted protein sequences of PtDXS and PtDXR differ from other related protein sequences, but the functional domain was similar to those found in other species. Multiple alignment analyses suggested that the domain is highly conserved and plays a key role in the activities of the enzymes.

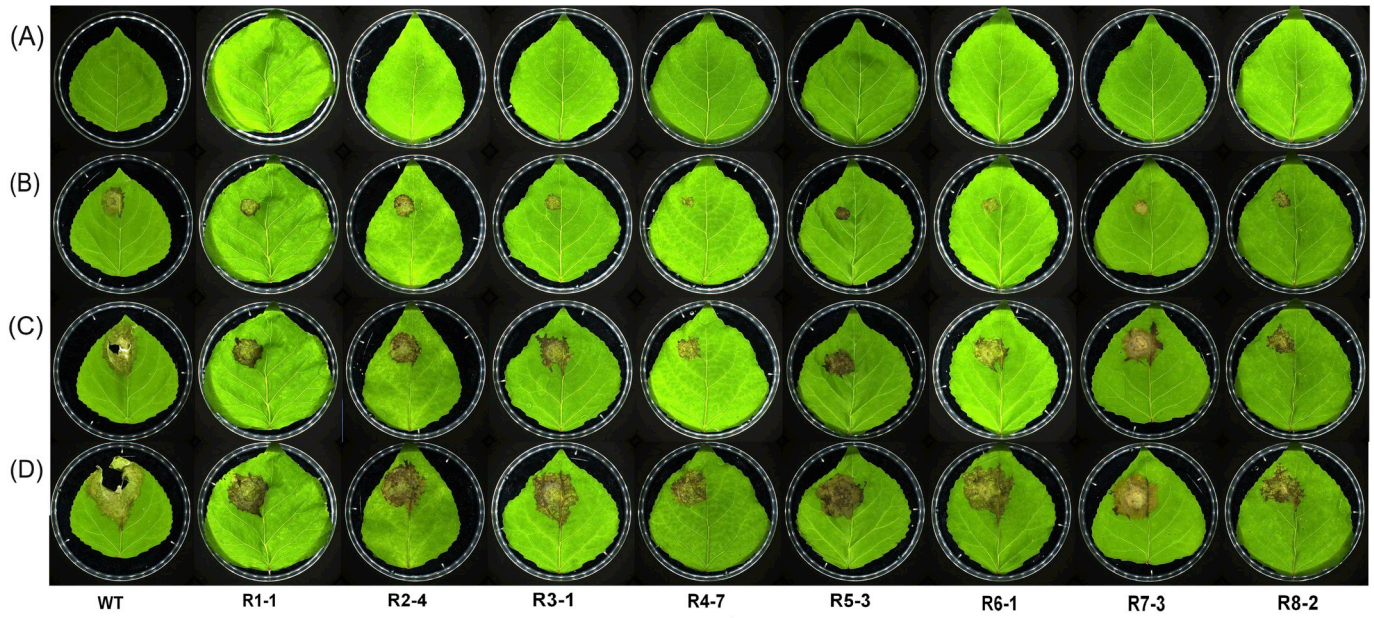

Fig. 9. Time-course and necrotic symptom analysis of WT and PtDXR transgenic plants during defense against *Septotis populiperda*. (A) Leaves of WT and PtDXR transgenic plants before inoculation with the pathogen. (B–D) Plaque index necrotic symptom analysis of WT and PtDXR transgenic plants 1 day (B), 2 days (C), and 3 days (D) following inoculation with the pathogen. Three independent experiments were performed.

Color complementation assays are commonly used to confirm the functions of the DXR and DXS enzymes, as the pAC-LYC plasmid includes all of the functional genes for β-carotene synthesis (Misawa et al., 1995; Cunningham et al., 1994; Blas et al., 2010) and can increase the yield of lycopene, and consequently the colonies display a pink color (Yang et al., 2012). However, in this study, we used the more advanced technique of HPLC–MS/MS to determine the activities of the PtDXR and PtDXS enzymes. HPLC–MS/MS demonstrated that the isolated expression product of the *PtDXS* gene was able to catalyze the reaction of pyruvic acid and fructose-1,6-bisphosphate to form DXP, and that the purified product of PtDXR can catalyze the formation of MEP from DXP.

PtDXS and PtDXR expression varied slightly among all tissues evaluated, with higher PtDXS expression in young leaves than in other organs, while the highest expression levels of PtDXR were in young leaves, and the lowest expression levels in roots. Tissue expression could be used as a mechanism for regulating the supply of MEP to biosynthetic pathways localized in these plant parts. To elucidate the expression patterns of PtDXS and PtDXR in different environments, we simulated different conditions, with 200 mM NaCl, 10% PEG_{6000}, and

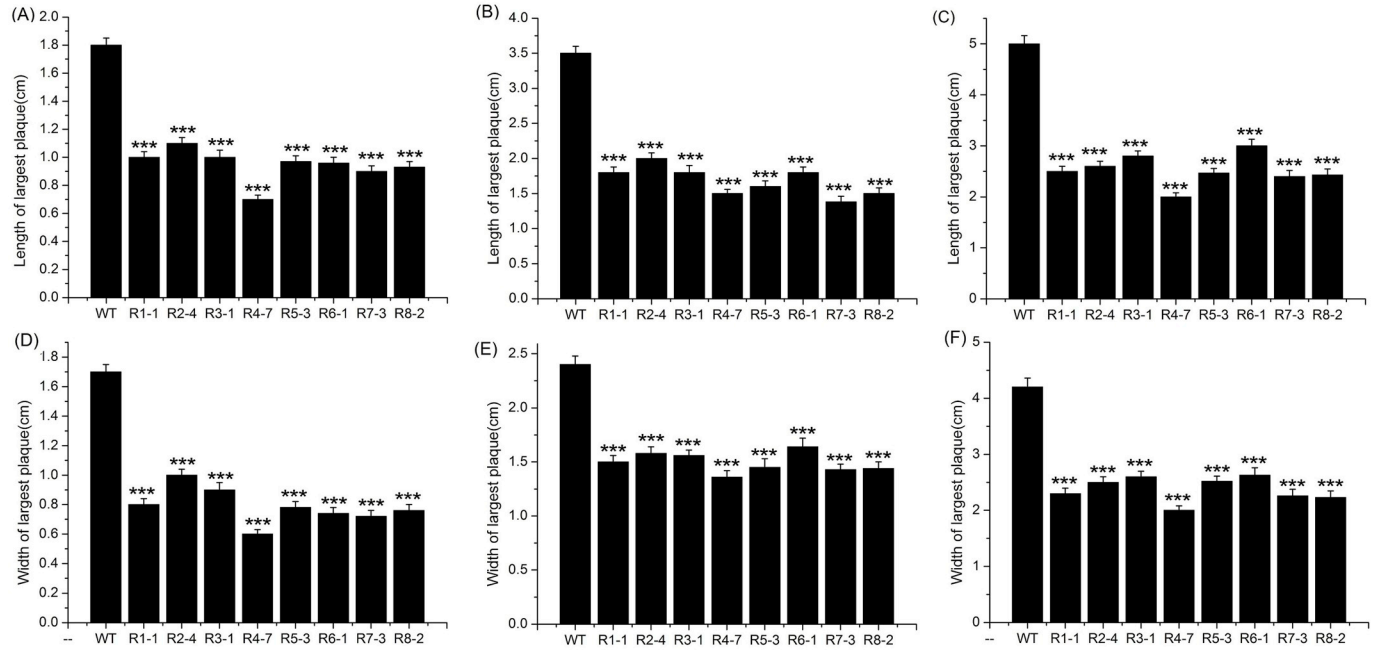

Fig. 10. Length and width analyses of the largest plaque in WT and PtDXR transgenic plants following pathogen inoculation. (A–C) Length of the largest plaque of WT and PtDXR transgenic plants 1 day (A), 2 days (B), and 3 days (C) following inoculation with the pathogen. (D–F) Width of the largest plaque of WT and PtDXR transgenic plants 1 day (D), 2 days (E), and 3 days (F) following inoculation with the pathogen. Three independent experiments were performed. All values are expressed as means ± SD.

200 μM ABA as salt-, drought-, and hormone-stress treatments, respectively. The results of these experiments indicated that PtDXS and PtDXR play significant roles in the regulation of stress conditions and participate in a variety of physiological responses.

Previous studies have reported that DXS exhibited diurnal changes (Dudareva et al., 2005) while diurnal changes in the transcript level of DXR were observed only in certain plants (Loivamaki et al., 2007). According to the observed periodic pattern, we determined that the *PtDXS* gene exhibits diurnal variation, whereas PtDXR exhibited no diurnal variation. Wiberley et al. (2009) described the relationships between isoprene and various genes in the MEP pathway, but we only analyzed the diurnal variations in *DXS* and *DXR* gene expression; the changes in isoprene content were not assessed. In addition, Expression of the *PtDXS* gene was higher under light compared with dark conditions, an 7-fold difference in the DXS expression level was seen between light and dark conditions. We speculate that the *PtDXS* gene is also dependent on the photoperiod.

Tomohisa et al. cloned the *DXR* gene from Synechocystis and overexpressed it in tobacco. They found no difference in growth between the transgenic and WT tobacco plants, but the levels of chlorophyll and anthraquinones such as sulfanil, solanesol, β-sitosterol, and β-carotene were significantly higher in the transgenic tobacco. Plants synthesize a large number of isoprenoid compounds that are very diverse in structure and function. Some isoprenoids are essential in all plants. For instance, chlorophylls and carotenoids are required as photosynthetic pigments, ubiquinone and plastoquinone as electron carriers, sterols as structural components of membranes, dolichols as oligosaccharide donors in protein glycosylation, and abscisic acid, brassinosteroids, cytokinins, and gibberellins as growth regulators. In this study, we found that the phenotype, including shoot height, stem diameter, number of leaves, and leaf area of the poplars, was better in WT poplar. Generally, carotenoid genes are upregulated under high-salt, high-light, N-deficient, and other stress conditions. Our study demonstrated significantly higher levels of SOD, CAT, and POD in poplars overexpressing *PtDXR* than in WT poplars. Many methods of improving disease resistance in plants have been suggested, but there are no reports that overexpression of *DXR* can improve disease resistance. In this study, overexpression of *PtDXR* in Nanlin895 poplar improved the plant's resistance to *S. populiperda* infection, which is significant for breeding resistant poplars.

In conclusion, we cloned two full-length genes encoding PtDXS and PtDXR, which are involved in the biosynthesis of isoprenoids in *P. trichocarpa*. We also identified the catalytic functions of the enzymes encoded by these genes. We analyzed the expression patterns of PtDXS and PtDXR in various tissues, and confirmed the expression levels of PtDXS and PtDXR under multiple abiotic stresses. The expression profiles of PtDXS and PtDXR were determined at different times, revealing that the *PtDXS* gene exhibits diurnal changes, whereas the *PtDXR* gene does not. This correlation further confirmed that PtDXS and PtDXR are important enzymes responsible for the biosynthesis of isoprenoids in *P. trichocarpa*. Thus, overexpression of PtDXR enhances growth and tolerance to abiotic and biotic stresses in transgenic poplar.

Acknowledgments

This work was supported by the National Key Program on Transgenic Research(2018ZX08020002), the National Science Foundation of China (No. 31570650) and the Priority Academic Program Development of Jiangsu Higher Education Institutions.

Appendix A. Supplementary data

Supplementary data related to this article can be found at https://doi.org/10.1016/j.plaphy.2019.05.034.

Conflicts of interest

The authors declare no conflicts of interest.

References

Blas, A.L., Ming, R., Liu, Z., Veatch, O.J., Paull, R.E., Moore, P.H., et al., 2010. Cloning of the papaya chromoplast-specific lycopene β-cyclase, cpcyc-b, controlling fruit flesh color reveals conserved microsynteny and a recombination hot spot. Plant Physiol. 152 (4), 2013–2022.

Carreteropaulet, L., Ahumada, I., Cunillera, N., RodríGuezconcepción, M., Ferrer, A., Boronat, A., et al., 2002. Expression and molecular analysis of the Arabidopsis DXR gene encoding 1-deoxy-d-xylulose 5-phosphate reductoisomerase, the first committed enzyme of the 2-c-methyl-d-erythritol 4-phosphate pathway. Plant Physiol. 129 (4), 1581–1591.

Cordoba, E., Porta, H., Arroyo, A., San, R.C., Medina, L., Rodríguezconcepción, M., et al., 2011. Functional characterization of the three genes encoding 1-deoxy-d-xylulose 5-phosphate synthase in maize. J. Exp. Bot. 62 (6), 2023–2038.

Cunningham, F.X., Gantt, E., 1994. Molecular structure and enzymatic function of lycopene cyclase from the cyanobacterium Synechococcus sp strain PCC7942. Plant Cell 6 (8), 1107–1121. https://doi.org/10.2307/3869889.

Dudareva, N., Andersson, S., Orlova, I., Gatto, N., Reichelt, M., Rhodes, D., Boland, W., Gershenzon, J., 2005. The nonmevalonate pathway supports both monoterpene and sesquiterpene formation in snapdragon flowers. Proc. Natl. Acad. Sci. U.S.A. 102 (3), 933.

Eisenreich, W., Schwarz, M., Cartayrade, A., Arigoni, D., Zenk, M.H., Bacher, A., 1998. The eoxyxylulose phosphate pathway of terpenoid biosynthesis in plants and microorganisms. Chem. Biol. 5 (9), 221–233.

Eisenreich, W., Bacher, A., Arigoni, D., Rohdich, F., 2004. Biosynthesis of isoprenoids via the non-mevalonate pathway. Cellular & Molecular Life Sciences Cmls 61 (12), 1401–1426.

Enfissi, E.M.A., Fraser, P.D., Lois, L.M., Boronat, A., Schuch, W., Bramley, P.M., 2005. Metabolic engineering of the mevalonate and non-mevalonate isopentenyl diphosphate-forming pathways for the production of health-promoting isoprenoids in tomato. Plant Biotechnology Journal 3 (1), 17–27.

Estévez, J.M., Cantero, A., Reindl, A., Reichler, S., León, P., 2001. 1-Deoxy-d-xylulose-5-phosphate synthase, a limiting enzyme for plastidic isoprenoid biosynthesis in plants. J. Biol. Chem. 276 (25), 22901–22909.

Floss, D.S., Hause, B., Lange, P.R., KäSter, H., Strack, D., Walter, M.H., 2010. Knock-down of the mep pathway isogene 1-deoxy-d-xylulose 5-phosphate synthase 2 inhibits formation of arbuscular mycorrhiza-induced apocarotenoids, and abolishes normal expression of mycorrhiza-specific plant marker genes. Plant J. 56 (1), 86–100.

Gong, Y., Liao, Z., Chen, M., Zuo, K., Guo, L., Tan, Q., et al., 2005. Molecular cloning and characterization of a 1-deoxy-d-xylulose 5-phosphate reductoisomerase gene from ginkgo biloba. DNA Sequence 16 (2), 111–120.

Hans, J., Hause, B., Strack, D., Walter, M.H., 2004. Cloning, characterization, and immunolocalization of a mycorrhiza-inducible 1-deoxy-d-xylulose 5-phosphate reductoisomerase in arbuscule-containing cells of maize. Plant Physiol. 134 (2), 614–624.

Henriquez, M.A., Soliman, A., Li, G., Hannoufa, A., Ayele, B.T., Daayf, F., 2016. Molecular cloning, functional characterization and expression of potato (*Solanum tuberosum*) 1-deoxy-d-xylulose 5-phosphate synthase 1 (*StDXS1*) in response to *Phytophthora infestans*. Plant Sci. 243, 71–83.

Khemvong, S., Suvachittanont, W., 2005. Molecular cloning and expression of a cDNA encoding 1-deoxy-d-xylulose-5-phosphate synthase from oil palm Elaeis guineensis Jacq. Plant Sci. 169 (3), 571–578.

Lange, B.M., Croteau, R., 1999. Isoprenoid biosynthesis via a mevalonate-independent pathway in plants: cloning and heterologous expression of 1-deoxy-d-xylulose-5-phosphate reductoisomerase from peppermint. Arch. Biochem. Biophys. 365 (1), 170–174.

Lange, B.M., Rujan, T., Martin, W., Croteau, R., 2001. Isoprenoid biosynthesis: the evolution of two ancient and distinct pathways across genomes. Proc. Natl. Acad. Sci. U. S. A. 97 (24), 13172–13177.

Lange, B.M., Wildung, M.R., Mccaskill, D., Croteau, R., 1998. A family of transketolases that directs isoprenoid biosynthesis via a mevalonate-independent pathway. Proc. Natl. Acad. Sci. U.S.A. 95 (5), 2100–2104.

Li, C.W., Su, R.C., Cheng, C.P., Sanjaya, You, S.J., Hsieh, T.H., et al., 2011. Tomato RAV transcription factor is a pivotal modulator involved in the AP2/EREBP-mediated defense pathway. Plant Physiol. 156 (1), 213–227.

Lichtenthaler, H.K., 1999. The 1-deoxy-d-xylulose-5-phosphate pathway of isoprenoid biosynthesis in plants. Annu. Rev. Plant Physiol. Plant Mol. Biol. 50 (50), 47.

Lois, L.M., Rodríguez-Concepción, M., Gallego, F., Campos, N., Boronat, A., 2010. Carotenoid biosynthesis during tomato fruit development: regulatory role of 1-deoxy-d-xylulose 5-phosphate synthase. Plant J. 22 (6), 503–513.

Loivamäki, M., Louis, S., Cinege, G., Zimmer, I., Fischbach, R.J., Schnitzler, J.P., 2007. Circadian rhythms of isoprene biosynthesis in grey poplar leaves. Plant Physiol. 143 (1), 540–551.

Misawa, N., Satomi, Y., Kondo, K., Yokoyama, A., Kajiwara, S., Saito, T., et al., 1995. Structure and functional analysis of a marine bacterial carotenoid biosynthesis gene cluster and astaxanthin biosynthetic pathway proposed at the gene level. J. Bacteriol. 177 (22), 6575–6584.

Morrone, D., Lowry, L., Determan, M.K., Hershey, D.M., Xu, M., Peters, R.J., 2010. Increasing diterpene yield with a modular metabolic engineering system in *E. coli*: comparison of MEV and MEP isoprenoid precursor pathway engineering. Appl.

Microbiol. Biotechnol. 85 (6), 1893–1906.
Movahedi, A., Zhang, J., Gao, P., Yang, Y., Wang, L., Yin, T., et al., 2015. Expression of the chickpea carnac3, gene enhances salinity and drought tolerance in transgenic poplars. Plant Cell Tissue Organ Cult. 120 (1), 141–154.
Murashige, T., Skoog, F., 2010. Murashige and Skoog Medium.
Peebles, C.A.M., Sander, G.W., Hughes, E.H., Peacock, R., Shanks, J.V., San, K.Y., 2011. The expression of 1-deoxy-d-xylulose synthase and geraniol-10-hydroxylase or anthranilate synthase increases terpenoid indole alkaloid accumulation in *Catharanthus roseus*, hairy roots. Metab. Eng. 13 (2), 234–240.
Rohmer, M., 1999. The discovery of a mevalonate-independent pathway for isoprenoid biosynthesis in bacteria, algae and higher plants. Nat. Prod. Rep. 16 (5), 565.
Sambrook, J., Fritsch, E.F., Maniatis, T., 1989. Detection and analysis of proteins expressed from cloned genes. In: Sambrook, J. (Ed.), Molecular Cloning: A Laboratory Manual, second ed. Cold Spring Harbor Laboratory Press, New York, pp. 18.1–18.85.
Shen, G., Pang, Y., Wu, W., Liao, Z., Zhao, L., Sun, X., et al., 2006. Cloning and characterization of a root-specific expressing gene encoding 3-hydroxy-3-methylglutaryl coenzyme a reductase from *Ginkgo biloba*. Mol. Biol. Rep. 33 (2), 117.
Tong, Y., Su, P., Zhao, Y., Zhang, M., Wang, X., Liu, Y., et al., 2015. Molecular cloning and characterization of DXS and DXR genes in the terpenoid biosynthetic pathway of Tripterygium wilfordii. Int. J. Mol. Sci. 16 (10), 25516–25535.
Walter, M.T., Strack, D., 2010. Arbuscular mycorrhizal fungi induce the non-mevalonate methylerythritol phosphate pathway of isoprenoid biosynthesis correlated with accumulation of the 'yellow pigment' and other apocarotenoids. Plant J. 21 (6), 571–578.
Wiberley, A.E., Donohue, A.R., Westphal, M.M., Sharkey, T.D., 2010. Regulation of isoprene emission from poplar leaves throughout a day. Plant Cell Environ. 32 (7), 939–947.
Wu, S.J., Shi, M., Wu, J.Y., 2009. Cloning and characterization of the 1-deoxy-d-xylulose 5-phosphate reductoisomerase gene for diterpenoid tanshinone biosynthesis in *Salvia miltiorrhiza* (Chinese sage) hairy roots. Biotechnol. Appl. Biochem. 52 (1), 89–95.
Wungsintaweekul, J., Sirisuntipong, T., Kongduang, D., Losuphanporn, T., Ounaroon, A., Tansakul, P., et al., 2008. Transcription profiles analysis of genes encoding 1-deoxy-d-xylulose 5-phosphate synthase and 2c-methyl-d-erythritol 4-phosphate synthase in plaunotol biosynthesis from *Croton stellatopilosus*. Biol. Pharm. Bull. 31 (5), 852.
Xiang, S., Usunow, G., Lange, G., Busch, M., Tong, L., 2007. Crystal structure of 1-deoxy-d-xylulose 5-phosphate synthase, a crucial enzyme for isoprenoids biosynthesis. J. Biol. Chem. 282 (4), 2676–2682.
Xu, Y., Liu, J., Liang, L., Xin, Y., Zheng, Z., Gao, Z., et al., 2014. Molecular cloning and characterization of three cDNAs encoding 1-deoxy-d-xylulose-5-phosphate synthase in Aquilaria sinensis (Lour.) Gilg. Plant Physiol. Biochem. 82 (3), 133–141.
Yang, J., Adhikari, M.N., Liu, H., Xu, H., He, G., Zhan, R., et al., 2012. Characterization and functional analysis of the genes encoding 1-deoxy-d-xylulose-5-phosphate reductoisomerase and 1-deoxy-d-xylulose-5-phosphate synthase, the two enzymes in the MEP pathway, from Amomum villosum lour. Mol. Biol. Rep. 39 (8), 8287–8296.
Yao, H., Gong, Y., Zuo, K., Ling, H., Qiu, C., Zhang, F., et al., 2008. Molecular cloning, expression profiling and functional analysis of a DXR gene encoding 1-deoxy-d-xylulose 5-phosphate reductoisomerase from *Camptotheca acuminata*. J. Plant Physiol. 165 (2), 203–213.
Zhang, M., Li, K., Zhang, C., Gai, J., Yu, D., 2009. Identification and characterization of class 1 DXS gene encoding 1-deoxy-d-xylulose-5-phosphate synthase, the first committed enzyme of the MEP pathway from soybean. Mol. Biol. Rep. 36 (5), 879–887.